

Numerical simulation on Taylor dispersion enabled micromixture

Yang Yang · Jing Liu

Received: 20 February 2008
© Springer-Verlag 2008

Abstract In this paper, a brief discussion on microfluidic devices and micromixer were made to clarify the difficult issues and category thus encountered. Based on Taylor dispersion mechanism, a new kind of micromixing pattern was investigated. Theoretical hydrodynamics model was established to characterize the Taylor dispersion behavior of the micro fluid. Numerical simulation and parametric evaluation were performed on the micromixing pattern enabled by the time-interleaved segmentation feeding of fluid. And good mixing efficiency was obtained. The present research is expected to be of important reference for better understanding the Taylor micromixing process. The corresponding method thus developed can serve as a useful tool for designing future micromixer.

List of Symbols

c_k	mass fraction for phase k
\mathbf{F}	body force, N
n	number of phase
t	time, s
α_k	volume fraction of phase k
μ_k	viscosity of phase k , kg/m · s

Y. Yang · J. Liu (✉)
Technical Institute of Physics and Chemistry,
Chinese Academy of Sciences,
P.O. Box 2711, 100080 Beijing, China
e-mail: jliu@cl.cryo.ac.cn

Y. Yang
Graduate School, Chinese Academy of Sciences,
100080 Beijing, China

J. Liu
Department of Biomedical Engineering, School of Medicine,
Tsinghua University,
100084 Beijing, China

μ_m	viscosity of the mixture, kg/m · s
\mathbf{v}_k	velocity of phase k , m/s
\mathbf{v}_m	mass-average velocity, m/s
ρ_m	mixture density, kg/m ³
$\mathbf{v}_{dr,k}$	drift velocity for secondary phase k , m/s

Subscripts

k	phase
m	phase
p	phase
E	ethanol
w	water

1 Introduction

Microfluidic analytical chips designed for biological and chemical applications have attracted considerable attentions in the past decade [1–3]. Many modern biotechnology and chemistry have been benefited from this miniaturization trend [4]. The microfluidic analytical chip is not only capable of performing multiple procedures, e.g., sample handling, mixing, pretreatment, chemical reaction and separation [1], but also can offer several advantages, such as having smaller reagent volumes, shorter reaction times, higher selectivity and yield, fewer byproducts, increased process safety, possibility of parallel operations and automation and the promise of integrating an entire laboratory onto a single chip [4, 5]. That's why it was now widely called as "Lab-on-a-Chip".

For many Lap-on-a-Chip applications, rapid and homogenous mixing of two or more fluid species is inevitable [6–9] and has been one of the most challenging tasks the microfluidic analytical devices have to fulfill [10].

However, below the millimeter length scale, flow is not only laminar but also viscosity-dominated, which make the molecular diffusion a major mechanism for mixing [11]. Such diffusive mixing is generally rather slow and therefore requires a long mixing channel and mixing time to achieve the desirable mixture.

Up to now, a great many efforts have been made to improving performance of micromixer and numerous micromixer devices based on various mechanisms have been developed [6]. It is generally accepted that the most common technique for enhancing mixing is reducing the diffusion path between solvent and solute [12]. In terms of the applied methods, micromixer can be categorized as active and passive one. The former device enhances mixing by stirring the flow streams so as to create a secondary flow which stretches and folds the material lines to reducing the mixing path [1, 12] and therefore promoting the diffusive mixing effect. Although such micromixers can be activated on demand [4] and may effectively reduce the channel length and time required for mixing, most of them suffer from the difficulty to be integrated into microfluidic systems. Besides, they require external power source or internal mechanical moving parts [6]. That's why the active micromixer is often provided with expensive production cost and low mechanical stability [11].

As an alternative, many passive microfluidic mixers have also been intensively investigated in recent years. Parallel lamination and sequential lamination are two established methods for passive micromixer to reducing mixing path which parallel lamination is achieved by splitting the solute and solvent into sub streams and joining them in the mixing channel and sequential lamination is achieved by pushing the fluid through certain channel geometry [4, 12]. Although the passive micromixer usually appear more robust, easier to implement and can be easily integrated to the microfluidic system, the complex design of the microchannel makes the fabrication rather complicated and the efficiency of the mixing is still relatively low.

Recently, researchers turn to the "Taylor dispersion" (published by Geoffrey Taylor in 1953) to form a new pattern of passive micromixer [12–16]. The Taylor dispersion is a kind of phenomena that the solvent dispersed along the channel direction through a steady fluid flow. Its dispersion is caused by the combined convection parallel to the axis and molecular diffusion in the radial direction [17]. It has been proved that the effective diffusion coefficient of Taylor dispersion is much larger than that of the molecular diffusion [18–21]. Therefore, applying this mechanism to passive micromixer would provide great aid to improving mixing efficiency. Previously, nearly all investigation and analysis on Taylor dispersion were based on diffusion equation, rather than the hydrodynamic models which is however more real. Here, the hydrodynamic models were adopted

to carry out numerical simulation on the Taylor dispersion, aiming to provide a more strict theoretical interpretation on the process detail. Parametric evaluation was made on the micromixing pattern enabled by the time-interleaved segmentation of fluid.

2 Theoretical model

Mixing of two or more fluid species belongs to a kind of multiphase flow. Therefore one can adopt the classical Navier-Stokes equation and the corresponding multiphase continuity and momentum equation to characterize the mixture process. The mixture model as adopted in this paper is derived in the literature through applying various approaches [22]. It is assumed that one of the phases is a continuous fluid and the other phases are dispersed which can comprise of particles, bubbles or droplets. In this approach both the continuity equation and the momentum equation are written for the mixture of the continuous and dispersed phases. In addition, particle concentrations are solved from continuity equations for each dispersed phase. The momentum equations for the dispersed phases are approximated by algebraic equations. So the corresponding equations for the Taylor dispersion in the microchannel can be expressed as follows:

Continuity equation:

$$\frac{\partial}{\partial t}(\rho_m) + \nabla \cdot (\rho_m \mathbf{v}_m) = 0. \quad (1)$$

Momentum equation:

$$\begin{aligned} & \frac{\partial}{\partial t}(\rho_m \mathbf{v}_m) + \nabla \cdot (\rho_m \mathbf{v}_m \mathbf{v}_m) \\ &= -\nabla p + \nabla \cdot [\mu_m (\nabla \mathbf{v}_m + \nabla \mathbf{v}_m^T)] + \rho_m \mathbf{g} + \mathbf{F} \\ & \quad + \nabla \cdot \left(\sum_{k=1}^n \alpha_k \rho_k \mathbf{v}_{dr,k} \mathbf{v}_{dr,k} \right) \end{aligned} \quad (2)$$

where, \mathbf{v}_m is the mass-average velocity and $\mathbf{v}_m = \sum_{k=1}^n \alpha_k \rho_k \mathbf{v}_k / \rho_m$, ρ_m is the mixture density and $\rho_m = \sum_{k=1}^n \alpha_k \rho_k$, α_k is the volume fraction of phase k , ρ_k is the density of phase k , \mathbf{v}_k is the velocity of phase k , n is the number of phase. \mathbf{F} is a body force, and μ_m is the viscosity of the mixture $\mu_m = \sum_{k=1}^n \alpha_k \mu_k$, μ_k is the viscosity of phase k , $\mathbf{v}_{dr,k}$ is the drift velocity for secondary phase k and $\mathbf{v}_{dr,k} = \mathbf{v}_k - \mathbf{v}_m$.

This mixture model is a simplified multiphase model which uses a single-fluid approach. It can be used to model multiphase flows where the phases move at different velocities, but assume local equilibrium over short spatial length scale. The momentum equation is obtained by summing the individual momentum equations for all phases.

The relative velocity (also referred to as slip velocity) for the multiphase model can be expressed as the velocity of

a secondary phase (p) relative to the velocity of the primary phase (q):

$$\mathbf{v}_{pq} = \mathbf{v}_p - \mathbf{v}_q \quad (3)$$

The mass fraction for any phase (k) is expressed as:

$$c_k = \alpha_k \rho_k / \rho_m \quad (4)$$

The drift velocity and the relative velocity \mathbf{v}_{pq} are correlated by the following expression:

$$\mathbf{v}_{dr,p} = \mathbf{v}_{pq} - \sum_{k=1}^n c_k \mathbf{v}_{qk} \quad (5)$$

The volume fraction equation for the secondary phase reads as:

$$\frac{\partial}{\partial t}(\alpha_p \rho_p) + \nabla \cdot (\alpha_p \rho_p \mathbf{v}_m) = -\nabla \cdot (\alpha_p \rho_p \mathbf{v}_{dr,p}) \quad (6)$$

where, α_p is the volume fraction of the secondary phase p , ρ_p is the density of secondary phase p , \mathbf{v}_m is the mass-average velocity and $\mathbf{v}_{dr,p}$ is the drift velocity for secondary phase p .

3 Numerical simulation

Based on the above theoretical model, a comprehensive 2-D numerical simulation on the Taylor dispersion was developed by using the commercially available CFD software FLIENT. The calculation domain is prescribed in a $1000 \mu\text{m} \times 200 \mu\text{m}$ rectangle, where x denotes the channel length while y is the width of the channel (Fig. 1). Water and ethanol are selected as the two liquid to be mixed and water is set as primary phase and ethanol the secondary one. At the initial state, ethanol whose volume accounted for three–twenty of the total channel volume was sandwiched between the water. The boundary conditions are set as follows: the blue boundary stands for the velocity-inlet boundary condition which imitates the constant velocity of water; the red boundary is set as flow exit boundary condition and the flow-rate weighting at exit is 1. The other boundaries indicate the wall boundary condition.

In the calculation, the parameters of the two liquid are selected as follows: the density and viscosity of wa-

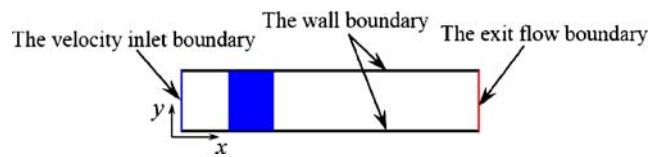


Fig. 1 Sketch of the calculation domains. The blue surface indicates the velocity-inlet boundary; the red surface indicates the exit flow boundary. The light blue 2-D domain is the initial ethanol space in the calculation; the white 2-D domain represents the initial water space in the calculation

ter are $\rho_w = 1000 \text{ kg/m}^3$, $\mu_w = 0.001003 \text{ kg/m} \cdot \text{s}$ respectively; and the density and viscosity of ethanol are $\rho_E = 790 \text{ kg/m}^3$, $\mu_E = 0.0012 \text{ kg/m} \cdot \text{s}$.

After completing the numerical simulation on the Taylor dispersion, another $10,000 \mu\text{m} \times 200 \mu\text{m}$ rectangle region is selected as the calculation domain for the micromixing pattern based on the time-interleaved segmentation. Water and ethanol are still chosen as the two liquid to be mixed and water is set as primary phase and ethanol is the secondary one. The setting of parameters and boundaries take the same as the above calculation except the velocity-inlet boundary condition which imitates constant velocity for water and ethanol alternate in periods. At the initial state, water is fully filled in the channel. Both typical behavior and parametric analysis on this micromixing pattern are implemented.

4 Result and discussion

4.1 Typical Taylor dispersion behavior

Figure 2 depicts the contour of density (mixture) for the typical Taylor dispersion in the $1000 \mu\text{m} \times 200 \mu\text{m}$ rectangle. The blue region represents the density of ethanol 790 kg/m^3 , and the red region delegates the density of water 1000 kg/m^3 . The other color region is the density of mixture. The velocity inlet of water is 0.001 m/s . With time goes on, the common boundary between the blue and red region begins to bend, the area of blue region is decreasing and the mixed region is growing larger. This is the phenomenon of convective diffusion parallel to the axis on the

Fig. 2 The contour of density (mixture) for the typical Taylor dispersion (kg/m^3)

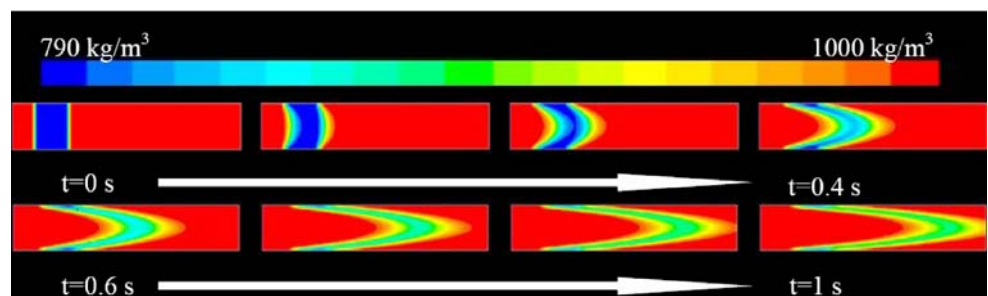
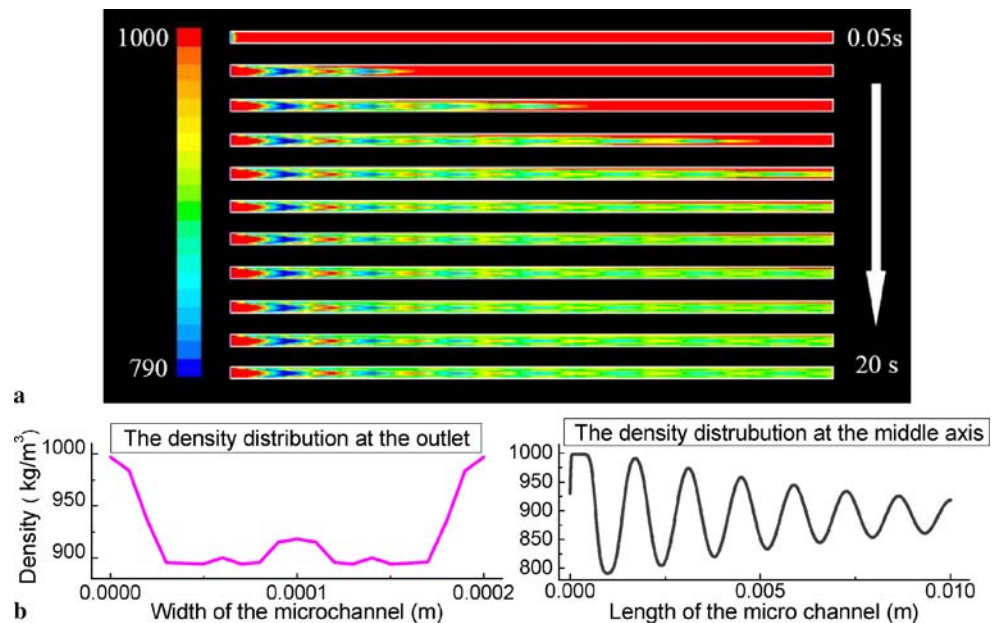


Fig. 3 The results for the typical micromixing pattern based on the time-interleaved segmentation. **a** The contour of density (mixture) for the typical micromixing pattern based on the time-interleaved segmentation (kg/m^3); **b** The density distribution at respectively the outlet boundary and along the middle axis at 20 s



common boundary between water and ethanol, namely the Taylor dispersion.

4.2 Typical micromixing pattern based on the time-interleaved segmentation

Figure 3a reflects the contour of density (mixture) for the typical micromixing pattern based on the time-interleaved segmentation in the $10,000 \mu\text{m} \times 200 \mu\text{m}$ rectangle. Uniformly, the blue region represents the density of ethanol, and the red region delegates the density of water. The other color region is the density of mixture. With time goes on, water and ethanol enter into the channel alternately in a period of 0.5 s with constant velocity 0.001 m/s and the Taylor dispersion takes on each common boundary consequently. Figure 3b is the final density distribution respectively at the outlet boundary and along the middle axis which takes on a “W” pattern and oscillatory distribution with gradually reducing amplitude.

In the calculation, the water and ethanol flow into the channel with identical velocity. Therefore, the mixing process is an equal-volume mixture and the final density should be $895 \text{ kg}/\text{m}^3$. From Fig. 3, it is evident that the density distribution in the channel is not the most homogenous until the mixing process lasts for 20 s. Accordingly, the following parametric analysis will be carried out to clarify that which way is the best to improve the mixing efficiency at the same period of 20 s.

4.3 Effect of velocity input on the mixture

The first parametric analysis is performed to validate the effect of velocity input on the micro mixture efficiency. The

calculation was carried out in two situations with identical or distinct velocity between the two phases of liquid.

4.3.1 Identical velocity between water and ethanol

When the two phases of liquid are feeding into the microchannel with identical velocity, the mixing process is an equal-volume mixture and the final density should be $895 \text{ kg}/\text{m}^3$. In order to test the mixing process in the whole channel with different velocity input, several values of velocity are prescribed respectively as 0.004 m/s, 0.002 m/s, 0.001 m/s and 0.0005 m/s. And the alternate period is set as 0.5 s and the mixing process last for 20 s. Figure 4 gives the results that a is the density distribution at the outlet boundary and b the density distribution along the middle axis. It is observed that when the velocity input is larger than 0.001 m/s, the density distribution at the outlet boundary is quite nonuniform and the amplitude of oscillatory density distribution along the middle axis keeps holding the line. When the velocity input is smaller than 0.001 m/s, the density distribution at the outlet boundary is quite homogenous and the amplitude of oscillatory density distribution along the middle axis is gradually decreasing and vanishes at last. Thus it can be seen that in the micro channel with same dimensions, the lower velocity input, the more homogenous mixture can be obtained in the same mixing time.

4.3.2 Distinct velocity between water and ethanol

Figure 5 depicts the results obtained by distinct velocity input between the two phases of liquid. For all the cases,

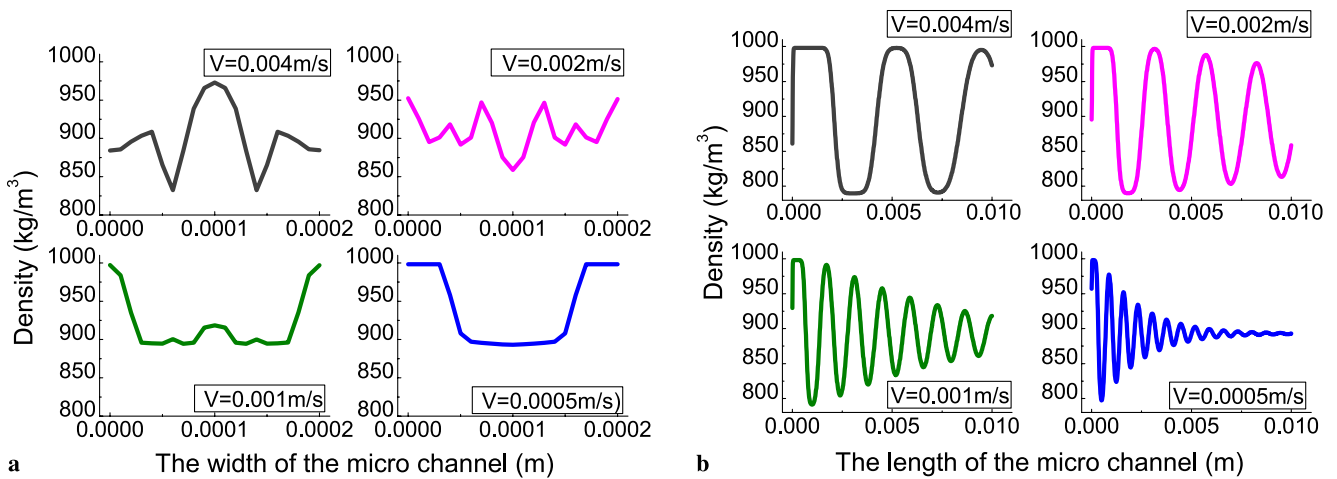
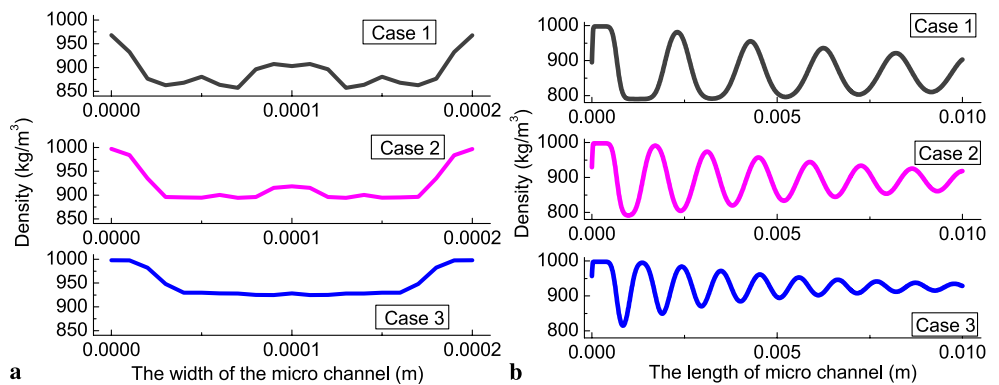


Fig. 4 The comparison result for the Sect. 4.3.1. **a** The density distribution along the outlet boundary at 20 s; **b** The density distribution along the middle axis at 20 s

Fig. 5 The comparison result for the Sect. 4.3.2. **a** The density distribution along the outlet boundary at 20 s; **b** The density distribution along the middle axis at 20 s



the velocity of water is assigned as 0.001 m/s; the alternate period is set as 0.5 s and the mixing process last for 20 s. From case 1 to 3, the velocity values of ethanol are 0.002 m/s, 0.001 m/s, and 0.0005 m/s respectively and the final homogenous mixed density should be 860 kg/m³, 895 kg/m³ and 930 kg/m³. As shown in Fig. 5, when the velocity of ethanol is less than the velocity of water, the density distribution at outlet is much more uniform and the amplitude of the oscillatory density distribution along the middle axis is gradually decreasing and vanishes at last. In other words, the mixture gets much more homogenous in the same mixing time.

4.4 Effect of alternate period on the mixture

After analyzing the affects of the velocity input, a further calculation adopting different alternate period values which are prescribed respectively as 1 s, 0.5 s, 0.2 s and 0.1 s is performed subsequently. The velocity input of both phases of liquid is set as 0.001 m/s and the mixing process lasts for 20 s. Figure 6 presents the result with a as the density distri-

bution at the outlet boundary and b the density distribution along the middle axis. It indicates that when alternate period is 1 s, the density distribution at outlet boundary is quite nonuniform and the amplitude of oscillatory density distribution along the middle axis keeps holding the line. When the alternate period is less than 0.5 s, namely 0.2 s and 0.1 s, the density distribution at the outlet boundary is much more homogenous and the amplitude of oscillatory density distribution along the middle axis is gradually decreasing and vanishes at last. Meanwhile, the decreasing speed of amplitude for alternate period 0.1 s is more rapid. So it can be concluded that the shorter the alternate period is the more homogenous mixture can be obtained in the whole channel with same mixing time.

4.5 Effect of fin-structure in the channel on the mixture

From all the above analysis, it can be seen that both low velocity input and short alternate period would improve the mixing efficiency. But it will cost longer time to obtain a volume of mixture with the low velocity. In order

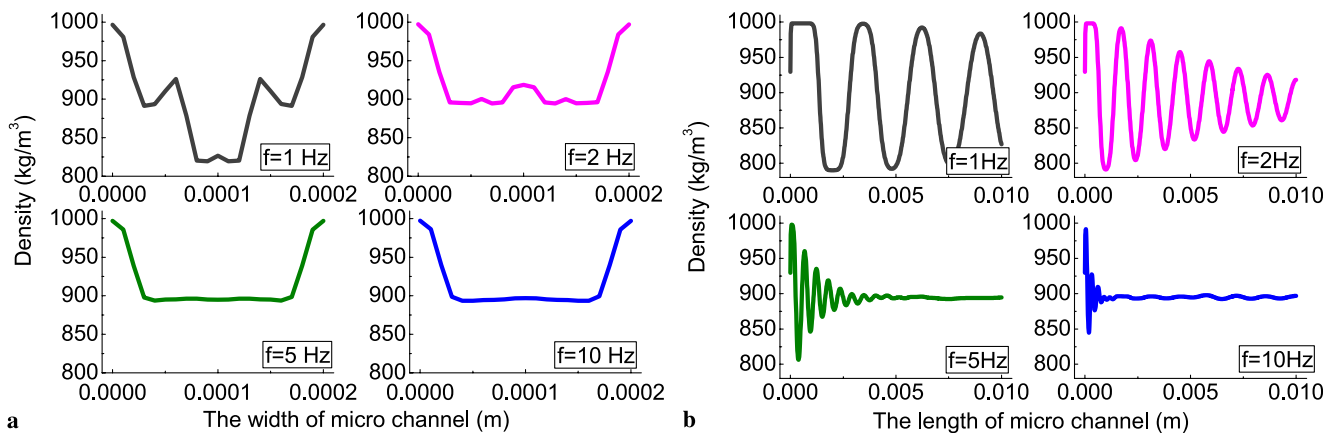
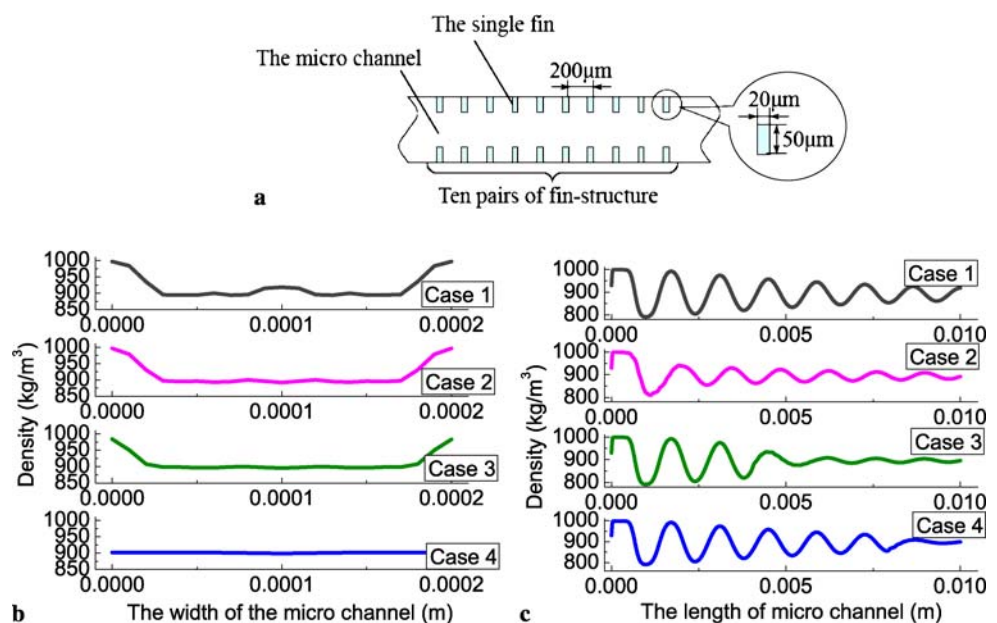


Fig. 6 The comparison result for the Sect. 4.4. **a** The density distribution along the outlet boundary at 20 s; **b** The density distribution along the middle axis at 20 s

Fig. 7 The comparison result for the Sect. 4.5. **a** The arrangement of the fin-structure; **b** The density distribution along the outlet boundary at 20 s; **c** The density distribution along the middle axis at 20 s



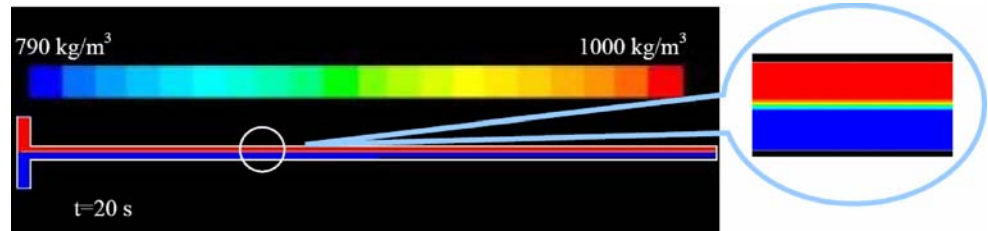
to achieve a shorter alternate period, a higher energy input is required. To improve this situation, we intentionally set some simple fin-structure into the channel, hoping to avoid such adverse factors. The dimension of a single fin is $50 \mu\text{m} \times 20 \mu\text{m}$; the interval distance between the two fins is $200 \mu\text{m}$ and there are 10 pairs of fins arranged symmetrically on both side of the micro channel, shown in Fig. 7a. For all the cases, the velocity of both phases of liquid is assigned as 0.001 m/s ; the alternate period is set as 0.5 s and the mixing process last for 20 s . Case 1 is arranged with no fin-structure, from case 2 to 4, the fin-structure is arranged at the sites of entrance, middle and the export respectively. Figure 7b and c display the result with b as the density distribution at outlet boundary and c as the density distribution along the middle axis. It represents that the density distri-

bution at outlet boundary is the most homogenous in case 4 and the density distribution along the middle axis is much more homogenous in case 3. Therefore, introduction of fin-structure to the hind half of the micro channel produces a marked effect on improving the mixture efficiency.

4.6 Discussion

As have mentioned before that nearly all previous investigation and analysis about Taylor dispersion and the micromixing pattern were developed from the diffusion equation. Adopting the hydrodynamic equations for the modeling would reveal more close to reality flow characteristics of Taylor dispersion, which could then help better understand the micromixing thus enabled.

Fig. 8 The contour of density (mixer) for the traditional micromixer in the T-channel (kg/m^3) at 20 s. The *blue region* is the density of ethanol, the *red region* is the density of water, and the *other color region* is the density of mixture



According to the calculation on the Taylor dispersion, the micromixing pattern based on the time-interleaved segmentation appears more efficient than that of a traditional mixing. One of such results for the traditional micromixer in the T-channel can be found as follows. For a comparison, utilizing the same mixture model and the volume of mixing part for the T-channel is chosen as equal to the micro channel as treated before, water and ethanol flow into the channel with a velocity 0.001 m/s and the mixing process lasts for 20 s. From Fig. 8, it is obvious that in the micro T-channel the mixture takes place only on the interface between the two liquid in a rather limited extent which is much weaker than the Taylor mixing pattern. This result not only indicated the similar molecular diffusion phenomenon but also strictly agrees with the conclusion that the effective diffusion coefficient of Taylor dispersion is far larger than the molecular diffusion. Therefore all the results prove that the molecular diffusion should also exists in the calculation on Taylor dispersion, even when the velocity approaches zero, furthermore the micromixing pattern as proposed in the present paper owns very promising future.

It should be mentioned that, the parametric analysis on the Taylor micromixing pattern is still limited. Many other influencing factors can in fact be determined by employing the numerical simulation method and considering more real situations, such as using various kinds of liquid, configurations of the fin-structure, variant interval distance and number of the fin-structure and so on.

5 Conclusion

In this paper, a comprehensive numerical simulation on the hydrodynamic behavior of Taylor dispersion under various typical physical parameters or structural configurations was accomplished. A relatively complete picture on the Taylor dispersion and micromixing pattern are revealed. The regularity on the mixed efficiency affected by different parameters has also been clarified. These results are of good reference for actual operation on the micromixing. The numerical simulation method as established in this paper can serve as a optimization tool for designing future micromixer.

Acknowledgement This work is partially supported by the NSFC Grant 50575219.

References

1. Fu LM, Yang RJ, Lin CH, et al. (2005) A novel microfluidic mixer utilizing electrokinetic driving forces under low switching frequency. *Electrophoresis* 5:1814–1824
2. John T, Mezić I (2007) Maximizing mixing and alignment of orientable particles for reaction enhancement. *Phys Fluids* 19:123602
3. Khatavkar VV, Anderson PD, Toonder JMJ, et al. (2007) Active micromixer based on artificial cilia. *Phys Fluids* 19:083605
4. Melin J, Giménez G, Roxhed N, et al. (2004) A fast passive and planar liquid sample micromixer. *Lab Chip* 4:214–219
5. Kim DJ, Oh HJ, Park TH, et al. (2005) An easily integrative and efficient micromixer and its application to the spectroscopic detection of glucose-catalyst reactions. *The Analyst* 130:293–298
6. Wu HY, Liu CH (2005) A novel electrokinetic micromixer. *Sens Actuators A* 118:107–115
7. Bisson C, Campbell J, Cheadle R, et al. (1998) A microanalytical device for the assessment of coagulation parameters in whole blood. In: *Proceedings of the Solid-State Sensor and Actuator Workshop*, Hilton Head, SC, pp 1–6
8. Anderson RC, Bogdan GJ, Puski A, et al. (1998) Genetic analysis systems: improvements and methods. In: *Proceedings of the Solid-State Sensor and Actuator Workshop*, Hilton Head, SC, pp 7–10
9. Kockmann N, Kiefer T, Engler M, et al. (2006) Convective mixing and chemical reactions in microchannels with high flow rates. *Sens Actuators B* 117:495–508
10. Niu XZ, Liu LY, Wen WJ, et al. (2006) Active microfluidic mixer chip. *Appl Phys Lett* 88:153508
11. Howell PB, Mott DR, Fertig S, et al. (2005) A microfluidic mixer with grooves placed on the top and bottom of the channel. *Lab Chip* 5:524–530
12. Nguyen NT, Huang XY (2005) Mixing in microchannels based on hydrodynamic focusing and time-interleaved segmentation: modeling and experiment. *Lab Chip* 5:1320–1326
13. Deshmukh LD, Pisano AP (2000) Continuous micromixer with pulsatile micropumps. *Technical Digest of the IEEE Solid State Sensors and Actuator Workshop*, Hilton Head Island, SC, USA, pp 73–76
14. Fujii T, Sando Y, Higashino K, et al. (2003) A plug and play microfluidic device. *Lab Chip* 3:193–197
15. Okamoto UT, Kitoh HO (2004) New methods for increasing productivity by using microreactors of planar pumping and alternating pumping types. *Chem Eng J* 101:57–63
16. Hong CC, Choi JW, Ahn CH (2004) A novel in-plane passive microfluidic mixer with modified Tesla structures. *Lab Chip* 4:109–113

17. Taylor GI (1953) Dispersion of soluble matter in solvent flowing slowly through a tube. *Proc R Soc London A* 219:186–203
18. Taylor GI (1954) Conditions under which dispersion of a solute in a stream of solvent can be used to measure molecular diffusion. *Proc R Soc London A* 225:473–477
19. Aris R (1956) On the dispersion of a solute in a fluid flowing through a tube. *Proc R Soc London A* 235:67–77
20. Barton NG (1983) On the method of moments for solute dispersion. *J Fluid Mech* 126:205–218
21. Brenner H, Edwards DA (1993) *Macrotransport Processes*, 1st ed. Butterworth-Heinemann, Boston, MA
22. Manninen M, Taivassalo V, Kallio S (1996) On the mixture model for multiphase flow, VTT Publications 288, Technical Research Center of Finland